Optical properties of phosphate glasses co-doped with Yb^{3+} and silver nanoparticles*

M. A. Vallejo H.[a], M. A. Martinez G.[a]†, A. V. Kiryanov[a], and J. L. Lucio M.[b]

[a] *Centro de Investigaciones en Óptica, Loma del Bosque* 115, *Col. Lomas del Campestre, León* 37150, *Guanajuato, México*
[b] *División de Ciencias e Ingenierías del Campus León de la Universidad de Guanajuato. Loma del Bosque* 103, *Col. Lomas del Campestre* 37150, *León Guanajuato, México*

(Received 24 April 2014; revised manuscript received 1 July 2014; published online 10 October 2014)

We report the fabrication and spectroscopic characterization of Yb^{3+}-doped phosphate glass, also containing silver nitrate. Scanning electron microscopy (SEM) provides the evidence of the formation of silver nano-particles (SNPs), which are formed as a consequence of melting and thermal decomposition of $AgNO_3$. Absorption spectra of the samples in the visible-to-near-infrared spectral range reveal the presence of bands centered at 410 nm associated with the SNP-plasmon resonance, and at 976 nm due to the Yb^{3+}. Under 916-nm laser-diode pumping, the effect of the SNP reflects that: i) the fluorescence in the 950-nm–1150-nm spectral range is strongly enhanced ($\sim$ 30 times), while the fluorescence decay time associated with the $^2F_{5/2} \rightarrow {}^2F_{7/2}$ transition of Yb^{3+} increases 25%, and ii) the basic lasing properties (saturation pumping intensity, the emission and absorption cross sections) are substantially improved.

Keywords: rare earths, phosphate glasses, silver nanoparticles

PACS: 42.70.−a, 78.20.−e, 81.05.Kf **DOI:** 10.1088/1674-1056/23/12/124214

1. Introduction

The study of Yb^{3+} ion embedded in different matrices has aroused much interest during the last decade.[1–7] This interest stems from the relevance of the Yb^{3+} spectroscopic properties for the development of lasers. The simplicity of the Yb^{3+} energy levels is the main characteristic since it can be approximated by a two-level system ($^2F_{7/2}$, $^2F_{5/2}$).[1] The emission and absorption cross sections, together with the fluorescence lifetime and the saturation pumping intensity are the properties relevant to characteristics of the material. However, these properties depend on the host material; thus, in fluoroborate glass an increase in the fluorescence centered at 975 nm is obtained as a consequence of the high Yb^{3+} concentration that the material can contain,[2] and similar results have been obtained to hold for niobosilicate and telurio-germanate glasses.[3] In the case of metaphosphate glasses, higher values of the emission and absorption cross sections[4] are achieved. It is important to remark that the ytterbium ion is also used as an active material in the construction of high efficiency fiber lasers in the 975 nm–1060 nm range.[5–7] Besides the increase of the emission cross section, the fluorescence decay time requires further optimization. Phosphate glass has been identified[8–15] as one of the most promising precursors of laser materials. As for the characteristics of the material, we should mention that it is soft and transparent from the ultraviolet (UV) to near infrared (IR), and relatively strong from the mechanical point of view. Phosphate glass also has a relatively high density (3 g/cm^3), high refractive index, and thermal conductivity, besides its high phonon energy.[16] The former property is welcome, for it is responsible for high emission efficiency in the infrared region. Moreover, phosphate glass is easy to prepare, in addition, it is versatile and can provide wide spectra of emission and absorption as compared with other crystalline materials.[17] Finally, it is worth mentioning that, as far as laser development is concerned, an advantage of phosphate glass over silicate glass is the possibility of doping with rare-earth concentration as high as 4×10^{21} cm^{-3},[18–20] without a noticeable deterioration of the technological properties of the glass and without luminescence quenching due to the formation of rare-earth clusters.

Our purpose in this work is to characterize the phosphate glasses co-doped with Yb^{3+} and SNP. Although, a detailed microscopic description of the phenomena involved in the system is beyond the scope of this work, we are interested in a phenomenological analysis of the influences of the silver nanoparticles on the properties of the glass, i.e., the spectroscopic effects and a quantitative measure of emission and absorption cross section, decay time, and the saturation pumping intensity (optical intensity corresponding to the saturation power per unit area). This information will be helpful in determining the potential use as laser material.

2. Experiment

Three glass samples were prepared (hereafter we refer to them as samples A, B, and C), whose compositions are $NaH_2PO_4H_2O$, Yb_2O_3, and $AgNO_3$ respectively (see Ta-

*Lucio M J L was financially supported by the CONACyT (Grant No. CB-2009-136186-F).
†Corresponding author. E-mail: mamg@cio.mx
© 2014 Chinese Physical Society and IOP Publishing Ltd

ble 1). It is convenient to remind that OH^- groups produce the quenching of ytterbium luminescence, that these OH groups are inevitably present in phosphate glasses, and its number increases as the Yb^{3+} concentration grows (see, for example, Refs. [21] and [22]) for that reason we work with a relatively low concentration of ytterbium in the core glass (0.5×10^{20} cm^{-3}). In the preparation process, the reagents were melted at 1050 °C for 4 hours in a porcelain crucible exposed to air. Then, the melt was poured in an aluminum-steel brass mold in open air and cooled down to room temperature. Afterwards, the samples were annealed at 450 °C for 2 hours in order to produce Ag metal nanoparticles. The SNPs were formed due to the thermal decomposition of $AgNO_3$ through the reaction: $2AgNO_3 = 2Ag(s) + 2NO_2(g) + O_2(g)$, where indices s and g denote gas and solid respectively. The glasses were then cut into a size of 10 mm in diameter and 6 mm in thickness, and polished.

Table 1. Glass composition in weight percentage (wt%).

Sample	$NaH_2PO_4H_2O$	Yb_2O_3	$AgNO_3$
Phosphate glass A	99.5	0.5	0.0
Phosphate glass B	95.5	0.5	4.0
Phosphate glass C	89.5	0.5	10.0

High resolution images of the samples are obtained from scanning electron microscopy (SEM: JOEL JSM-7401F). The result for sample C (with the highest SNP content) is shown in Fig. 1, the micrograph clearly demonstrates the presence of SNP. In Fig. 2 we report the results of the analysis of the area marked in Fig. 1. The horizontal axis shows the elements while the vertical axis the relative quantity of elements entering into the area analyzed. Figure 2 is not normalized, and the vertical axis is not shown completely either, otherwise the details of the weaker signals would be lost. From this figure we can learn that the silver signal is much stronger than the Yb one, and that an even weaker Si signal appears due to the use of porcelain crucibles in the preparing process.

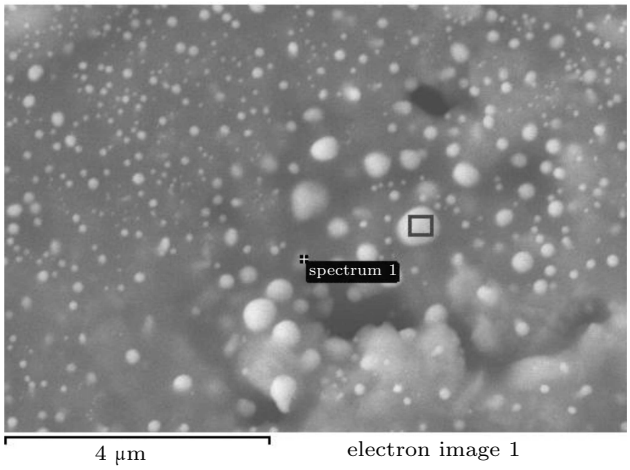


Fig. 1. SEM micrograph of sample C showing nano-particles. The analysis of the area marked with a square is reported in Fig. 2.

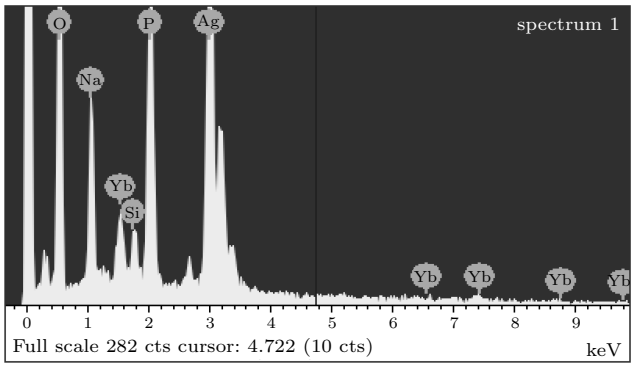


Fig. 2. Spectrum showing the amounts of element content in the area marked with a square in Fig. 1.

The spectral properties of the samples were obtained. On the one hand, using a 1-nm resolution Perkin–Elmer spectrophotometer, the absorption spectra of the samples at room temperature were recorded between 350 nm and 1100 nm. On the other hand, to obtain the emission spectra, an Ando AQ-6315A optical spectrum analyzer was used. In the latter case, we pumped the sample with a 200-mW semiconductor laser at 916 nm, and the detector was located in a line perpendicular to the excitation direction (to avoid the re-absorption effect). The absorption spectra are shown in Fig. 3, whereas the emission spectra are shown in Fig. 4. The lifetime of the near-IR fluorescence produced by the Yb^{3+} decay was measured in the same 90°-geometry, but in this case, the pump light from the 916-nm laser was modulated to give a square-wave signal (meander) on the sample. The luminescence (filtered) signal from the pumped sample was detected using an Si photodetector and processed by a computerized digital oscilloscope (Tektronix).

3. Results and discussion

From Fig. 3 one can conclude that as far as absorption is concerned, the behaviors of the three samples are similar: the main absorption band lies between 900 nm and 1000 nm, which is produced by the $^2F_{7/2} \rightarrow {}^2F_{5/2}$ (Yb^{3+}) transition. Note, however, that the absorption coefficient grows as the silver concentration in the samples increases. It is also worth noticing that the broad band centered at 410 nm appears for samples B and C, but no such band occurs in sample A. In the conventional interpretation,[23] the band is produced by the surface plasmon associated with the SNP. From the inset of Fig. 3, it is worth noticing that the tail of the plasmon reaches 1000 nm and, therefore, it enhances the Yb^{3+} absorption in the 950-nm–1000-nm range. This increase in the absorption at 916 nm produces an enhancement of the Yb^{3+} fluorescence (see below).

The emission spectra of the three samples under pumping at 916 nm are shown in Fig. 4, where included are a prominent peak at 977-nm and a less intense one at 1015 nm, both

of which are attributed to the $^2F_{5/2} \rightarrow {}^5F_{7/2}$ transition of the Yb^{3+} ion. Note that the fluorescence spectra we report start at 950 nm, so that the fluorescence produced by the SNP in the visible region is not included. Particularly relevant to this work are the changes observed in the infrared emission spectra, when the silver is included (samples B and C); in fact, the higher the silver content of the sample, the larger the enhancement of the fluorescence is. As the Yb^{3+} concentrations for the three samples are the same (refer to Table 1), these results suggest that the SNP concentration in the sample influences the populations of the $^2F_{7/2}$, $^2F_{5/2}$, and Yb^{3+} levels.

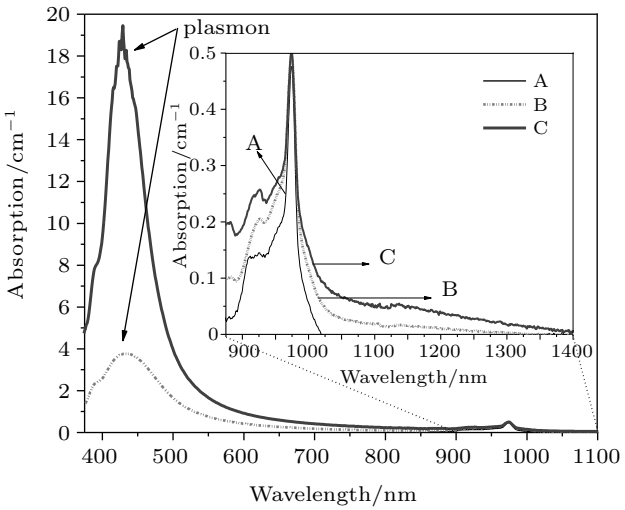


Fig. 3. Room temperature absorption spectra of the samples A (black thin solid line), B (gray dash–dotted line), and C (black thick solid line). The inset corresponds to an enlargement of the Yb^{3+} absorption band area.

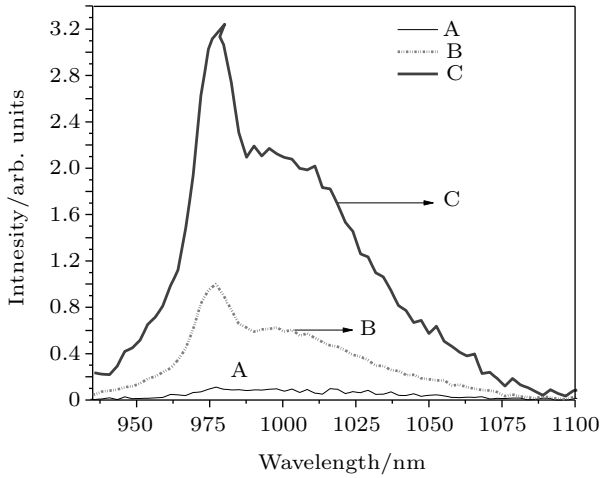


Fig. 4. Emission spectra of phosphate glasses co-doped with Yb^{3+} and SNP (samples A, B, and C) under 200-mW excitation at $\lambda = 916$ nm.

In Table 2 we report the decay time obtained from our measurements, and the comparisons with other authors' results are included. It is noticeable that τ grows as the SNP content in the samples increases; that is to say, the lifetimes of samples B and C deviate from the value obtained from sample A, the sample free of silver nitrate. It is known that the lifetime depends on the effective refractive index (n_{eff}) of the medium. We measured[24] the refractive indexes of the three samples and found to be $n^{\text{A}}{}_{\text{eff}} = 1.499$, $n^{\text{B}}{}_{\text{eff}} = 1.493$, and $n^{\text{C}}{}_{\text{eff}} = 1.475$. The trend of the lifetime values ($\tau^{\text{A}} < \tau^{\text{B}} < \tau^{\text{C}}$) can be roughly reproduced using the n_{eff} dependence predicted by Dolgaleva *et al.*[25]

Table 2. Lifetimes of fluorescence in the ~ 1 μm as measured from phosphate glasses co-doped with Yb^{3+} and SN.

Host	$N_{Yb}/10^{20}$ ions·cm^{-3}	τ/ms	Ref.
Phosphate glass	0.560	1.20	[4]
SACF 0.2	0.501	1.29	[1]
Phosphate glass A (0% SNP)	0.509	1.33	This work
Phosphate glass B (4% SNP)	0.509	1.50	This work
Phosphate glass C (10% SNP)	0.509	1.77	This work

Among the physical properties, the absorption cross section $\sigma_{\text{abs}}(\lambda)$, the emission cross section $\sigma_{\text{em}}(\lambda)$, and the saturation pumping intensity I_{sat}[1,2,4] (see below) serve as parameters to characterize materials suitable for laser development. Using the lifetimes reported in Table 2, we compute the spectral dependence of the cross sections from the following relations[26,27]

$$\sigma_{\text{em}}(\lambda) = \frac{\lambda^5 \eta}{8\pi c \tau n_{\text{eff}}^2} \frac{I\lambda}{\int \lambda I(\lambda)\,\mathrm{d}\lambda}, \tag{1}$$

$$\sigma_{\text{abs}}(\lambda) = \sigma_{\text{em}}(\lambda) \exp\left[\frac{h\nu - \varepsilon}{kT}\right], \tag{2}$$

where η represents the branching ratio for the radiative decay, n_{eff} is the refractive index of the glass host, c is the velocity of light, $I(\lambda)$ is the emission intensity of Yb^{3+} at wavelength λ (~ 975 nm), and ε is the temperature-dependent excitation energy, which is the net energy needed to excite an Yb^{3+} ion from the $^2F_{5/2}$ to the $^2F_{7/2}$ state at temperature T, h is the Planck constant, k is the Boltzmann's constant, and ν is the photon frequency. Assuming $\eta \sim 1$ for all samples, we obtain the stimulated emission $\sigma_{\text{em}}(\lambda)$ and absorption cross-section $\sigma_{\text{abs}}(\lambda)$ shown in Figs. 5 and 6 (see also Table 3).

The effects of silver on the behaviors of absorption and emission cross section are similar to the scenarios for the three samples and show interesting regularities. The following striking aspects of the absorption cross section are worth commenting (see Fig. 5): i) as the silver content of the sample increases, $\sigma_{\text{abs}}(\lambda)$ grows at 916 nm, and ii) in the first approximation, the silver effect on the absorption at 975 nm is small and negligible. For the emission cross section, the following points must be remarked: i) at 977 nm, the emission is larger when the sample includes silver, however, the difference in emission intensity between samples B and C is small, while the behavior at 1015 nm shows that the larger cross section corresponds to the sample free of SNP.

Table 3. Absorption and emission cross sections at 975 nm as obtained from phosphate glasses co-doped with Yb^{3+} and SNP.

Host	$N_{Yb}/10^{20}$ ions·cm^{-3}	$\sigma_{abs}(\lambda)/10^{-20}$ cm^2	$\sigma_{em}(\lambda)/10^{-20}$ cm^2	Reference
HMO	0.640	2.200	0.75	[13]
SACF0.2	0.501	1.190	0.98	[1]
Phosphate glass	0.560	1.400	1.00	[4]
Phosphate glass A (0%SNP)	0.509	0.930	0.78	This work
Phosphate glass B (4%SNP)	0.509	0.973	1.01	This work
Phosphate glass C (10%SNP)	0.509	0.974	1.05	This work

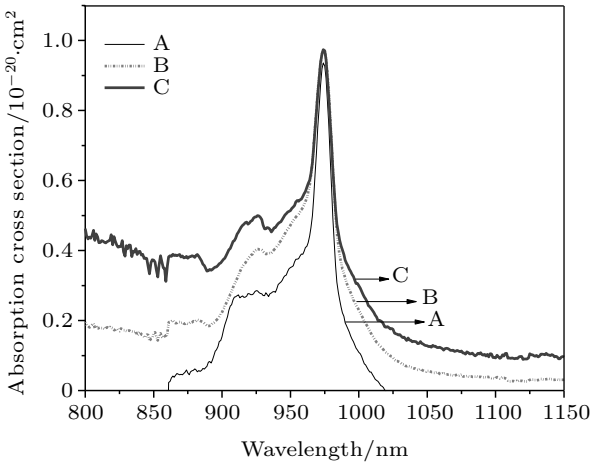


Fig. 5. Absorption cross sections of samples A (black thin solid line), B (gray dash–dotted line), and C (dark gray solid line).

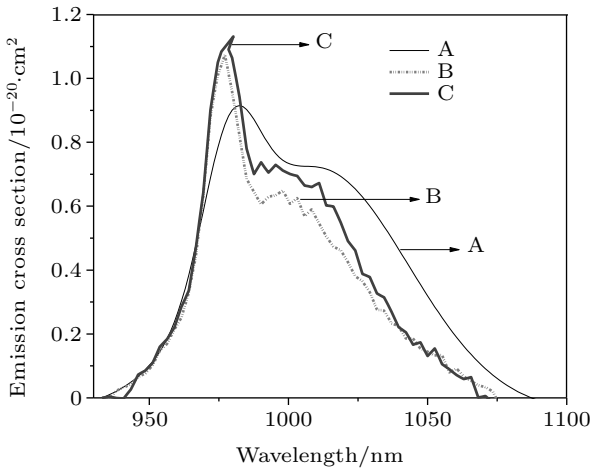


Fig. 6. Emission cross sections of samples A (black thin solid line), B (gray dash–dotted line), and C (dark gray solid line).

Further enhancement of the lasing properties of the materials at $\lambda = 975$ nm can be obtained from the saturation pumping intensity I_{sat}, which can be calculated from the following relation:[4,28]

$$I_{sat} = \frac{hc}{\lambda \sigma_{abs}(\lambda)\tau}. \quad (3)$$

Figure 7 shows the saturation pump intensity versus SNP concentration. We observe that a significant reduction of I_{sat} occurs as the SNP concentration is increased. In Table 4 we report the results for I_{sat} at $\lambda = 916$ nm (corresponding to an Yb^{3+} absorption peak). The consequence of incorporating the SNP is to reduce I_{sat}. For comparison, in Table 4 we also give the results of other authors. Note that in previous studies (see e.g. Refs. [15] and [27]), enhancement of I_{sat} is achieved by increasing the Yb^{3+} wt% content of the sample, however it is accompanied by a decrease of the fluorescence decay time τ, which in this context is an undesired effect. In contrast to previous approaches, in our case we keep the Yb^{3+} concentration constant and change solely the SNP concentration and still obtain improvement in the lasing properties of the material. Finally, note that the Yb^{3+}wt% we use is low in comparison with in the cases of oxy-fluoride silicate glasses,[1] fluorophosphates,[3] phosphosilicate,[29] silicate,[29] and phosphate.[29]

Table 4. Comparison of saturation pumping intensity (I_{sat}) between phosphate glasses co-doped with Yb^{3+} and SNP.

Host	Yb^{3+}/wt%	I_{sat}/(kW/cm^2)	Reference
SACF0.2	0.2	14.30	[1]
PSB	1	22.11	[29]
LSY	1	22.11	[29]
PNK	1	15.55	[29]
FP	0.3	20.91	[3]
Phosphate glass A (0%SNP)	0.5	16.37	This work
Phosphate glass B (4%SNP)	0.5	13.96	This work
Phosphate glass C (10%SNP)	0.5	11.82	This work

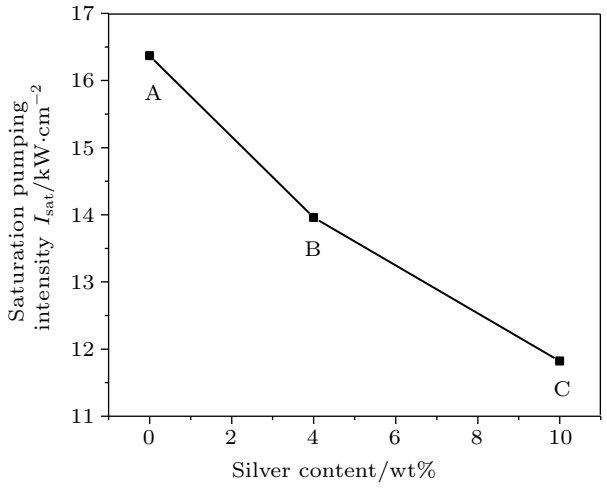


Fig. 7. Saturation pumping intensities of samples A, B and C with different amounts of the silver content.

4. Summary and conclusions

This work focuses on the spectral properties of phosphate glasses co-doped with Yb^{3+} and silver nitrate. We report the absorption and fluorescence spectra, as well as the absorption cross-section $\sigma_{abs}(\lambda)$, the emission cross-section $\sigma_{em}(\lambda)$, and the saturation pumping intensity I_{sat}. We conclude that the lasing properties of the material are improved when the silver concentration in the sample is increased (increase in $\sigma_{abs}(\lambda)$ and $\sigma_{em}(\lambda)$ and reduction of I_{sat}). We provide the evidence of the formation of silver nano-particles, and as far as interpretation is concerned, we can mention that most probably the silver produces a re-distribution of the populations between the Stark sublevels of the $^2F_{7/2}/^2F_{5/2}$ manifolds.

References

[1] Zhang Q, Ding J, Tang B, Cheng J, Qiao Y, Zhou Q, Qiu J, Chen Q and Chen D 2009 *J. Phys. D: Appl. Phys.* **42** 235405

[2] Kassab L R P, Tatumi S H, Morais A S, Courrol L C, Wetter N U and Salvador V L R 2001 *Opt. Express* **8** 585

[3] Jiang C, Zhang J Z, Deng P Z, Huang G S, Mao H F and Gan F X 1999 *Sci. China (Series E)* **42** 617

[4] Bell M J V, Quirinm W G, Oliveira S L, de Sousa D F and L Nunes A O 2003 *J. Phys.: Condens. Matter* **15** 4877

[5] Villegas I L, Cuadrado C, Díez A, Cruz J L, Martínez M A and Andrés M V 2011 *Laser Phys. Lett.* **8** 227

[6] Kuznetsov A G and Babin S A 2010 *Laser Phys.* **20** 1266

[7] Jacinto C, Oliveira S L, Nunes L A O, Catunda T and Bell M J V 2006 *J. Appl. Phys.* **100** 113103

[8] Liu H, Biswal S, Paye J, Nees J, Mourou G, Honninger C and Keller U 1999 *Opt. Lett.* **24** 917

[9] Paoloni S, Hein J, Tôpfer T, Walther H G, Sauerbrey R, Ehrt D and Wintzer W 2004 *Appl. Phys. B: Lasers Opt.* **78** 415

[10] Honninger C, Morier F, Moser M, Keller U, Brovelli L R and Harder C 1998 *Opt. Lett.* **23** 126

[11] Ehrmann P R and Campbell J H 2002 *J. Am. Ceram. Soc.* **85** 1061

[12] Ehrmann P R, Carlson K, Campbell J H, Click C A and Brow R K 2004 *J. Non-Cryst. Solids* **349** 105

[13] Courrol L C, Kassab L R P, Morais A S, Mendes C M S, Gomes L, Werrer N U, Vieira N D Jr, Cssanjes F C, Messaddeq Y and Ribeiro S J L 2003 *J. Lumin.* **102–103** 106

[14] Campbell J H and Suratwala T I 2000 *J. Non-Cryst. Solids* **263** 318

[15] Ebendorff H, Seeber W and Ehrt D 1995 *J. Non-Cryst. Solids* **183** 191

[16] Martínez M A, Kir'yanov A V, Lucio J L, Wiechers C and Kumar G A 2009 *J. Alloys Compd.* **473** 500

[17] Francini R, Giovenale F, Grassano U M, Laporta P and Taccheo S 2000 *Opt. Mater.* **13** 417

[18] Gapontsev V, Gapontsev D and Platonov N 2005 *Proc. CLEOIEurope-2005* (Munich, Germany, 2005) CJl-1-THU

[19] Denker B I, Galagan B I, Kamynin V A, Kurkov A S, Sadovnikova Ya E, Semenov S L, Sverchkov S E, Velmiskin V V and Dianov E M 2013 *Laser Phys. Lett.* **10** 1088

[20] Kühn S, Håkanson U, Rogobete L and Sandoghdar V 2006 *Phys. Rev. Lett.* **97** 017402

[21] Karlson G, Laurell F and Tellefsen J 2002 *Appl. Phys. B* **75** 41

[22] Bufetov I A, Semenov S L, Kosolapov A F, Mel′kumov M A, Dudin V V, Galagan B I, Denker B I, Osiko V V and Sverchkov S E, E M 2006 *Quantum Electron.* **36** 189

[23] Kalkmanan J L and Polman A 2005 *Appl. Phys. Lett.* **86** 041113

[24] Metricon Corporation, http://www.metricon.com/basic.html (accessed April 16, 2013)

[25] Dolgaleva K, Boyd R W and Milonni P W 2007 *J. Opt. Soc. Am. B* **24** 516

[26] Cruz S G, Martínez M A, Kir′yanov A V and Kumar G A 2005 *Opt. Mater.* **27** 1563

[27] France P W 1990 *Optical Fiber Laser and Amplifiers* (Blackie Glasgow and London) p. 28

[28] Ganeev R A and Ryasny A I 2006 *Appl. Phys. B* **84** 295

[29] Zou X and Toratani H 1995 *Phys. Rev. B* **52** 15889